

Critical behaviour of the four-dimensional spin glass in magnetic field

This article has been downloaded from IOPscience. Please scroll down to see the full text article.

1998 J. Phys. A: Math. Gen. 31 6355

(<http://iopscience.iop.org/0305-4470/31/30/005>)

View [the table of contents for this issue](#), or go to the [journal homepage](#) for more

Download details:

IP Address: 171.66.16.102

The article was downloaded on 02/06/2010 at 07:08

Please note that [terms and conditions apply](#).

Critical behaviour of the four-dimensional spin glass in magnetic field

Enzo Marinari[†], Carla Naitza[‡] and Francesco Zuliani[§]

Dipartimento di Fisica and INFN, Università di Cagliari, Via Ospedale 72, 09100 Cagliari, Italy

Received 26 February 1998

Abstract. We present numerical simulations of the four-dimensional Edwards Anderson Ising spin glass with binary couplings. Our results, in the midst of strong finite-size effects, suggest the existence of a spin-glass phase transition. We present a preliminary determination of critical exponents. We discuss spin-glass susceptibilities, cumulants of the overlap and energy overlap probability distributions, finite-size effects, and the behaviour of the disorder-dependent and integrated probability distributions.

1. Introduction

The Edwards–Anderson model of spin glasses [1] turns out, not astonishingly, to be hard to be understood. More surprisingly (at the start) also the Sherrington Kirkpatrick mean-field version of the model [2] appears to be very complex. Many unprecedented features appear: for example the (spin-glass) phase transition survives the presence of a finite magnetic field [3] under the de Almeida-Thouless (AT) line. The Parisi replica symmetry breaking (RSB) solution [4] appears to describe accurately the model in the low T broken phase (and it is believed to be the real solution of the model).

The relevant question is now trying to establish how many of the features of the Parisi solution survive when discussing finite-dimensional spin-glass models. For example the presence of a phase transition in a finite magnetic field, that is implied by the Parisi solution [4], is not compatible with the point of view of the *droplet model* [5], where one expects the transition to be removed from the action of a small magnetic field.

As usual in a complex theoretical scenario, numerical simulations try to play a part (for a review of recent simulations of spin-glass models see [6]). Here we will report numerical simulations that thermalize large lattices with a large number of samples: we will try to show many signatures hinting about the presence of a phase transition, and we will be plagued by large finite-size effects.

Numerical simulations of spin glasses with non-zero magnetic field are now well known. Maybe the first work on the subject is the one by Sourlas [7, 8]. The numerical simulations of [9, 10] (see also the criticism in [11] and the reply [12]) use the concept of energy overlap, that turns out to be very relevant in this study: these simulations give a first evidence, but the computers of the time allowed too small lattices for getting conclusive results. Simulations of [13] measure constant susceptibility curves [14], and detect the existence of an AT line.

[†] E-mail address: marinari@ca.infn.it

[‡] E-mail address: naitza@ca.infn.it

[§] E-mail address: zuliani@ca.infn.it

On the contrary, the work of [15] does not detect one, whilst [16–18] are more on the yes side. Again, the work of [19] is negative on the existence of a transition, while [20] claims the difficulty of establishing a firm conclusion (maybe a wise approach). Finally, recent numerical work using a dynamic approach has been able to claim, again, the existence of a clear transition to a spin glass phase [21, 22].

Here, as we will explain in the following sections, we will find evidence that we consider strongly suggestive of the existence of a phase transition, and we will present very preliminary determinations of critical exponents. We will also find that even on large lattices (on current standards) finite-size effects are dramatically strong, and we will discuss them in detail.

2. Numerical simulations

In this section we shall discuss the four-dimensional (4D) Edwards–Anderson spin-glass system [1] with bimodal quenched random couplings $J = \pm 1$. Our numerical simulations have been using the *parallel tempering* approach [23], which makes a real difference in the simulations of systems with quenched disorder. The interested reader will find for example in the last of [23] an introduction to optimized Monte Carlo methods (including tempering and, more in general, the multi-canonical approaches).

The model Hamiltonian is

$$H = - \sum_{(i,j)} \sigma_i J_{i,j} \sigma_j - h \sum_i \sigma_i \quad (1)$$

where the first sum runs over first neighbouring sites on a 4D lattice and the J are binary quenched random couplings. $\beta = 1/T$ is the inverse couplings that multiplies the Hamiltonian in the Boltzmann weight.

In table 1 we report the parameters relevant for our tempered simulations: for each lattice size we give the number of discarded thermalization sweeps and of the sweeps used for measurements, the total number of samples that we have analysed, the number of temperatures used in each tempered run (i.e. the number of copies of the system updated in parallel at different β values and among which the temperature values have been swapped), the temperature increment, the minimum and maximum temperatures.

We have taken a magnetic field $h = 0.4$. We know from former work that this value is large enough to make the transition clearly different from the $h = 0$ pure case, but not large enough to cross the AT line (for a more detailed discussion of this point see [21] and references therein).

The β values have been chosen, as customary and reasonable, in order to keep the acceptance factor of the tempering β swap of order $\frac{1}{2}$. In our case we have a β acceptance ratio close to 0.8 for $L = 3$ that goes down to a number close to 0.6 at $L = 9$.

Table 1. Parameters of the tempered Monte Carlo runs.

L	Thermalization	Equilibrium	Samples	N_β	δT	T_{\min}	T_{\max}
3	20 000	20 000	2560	19	0.1	1.0	2.8
5	80 000	80 000	1920	19	0.1	1.0	2.8
7	200 000	200 000	960	46	0.04	1.0	2.8
9	150 000	150 000	64	66	0.04	1.0	3.6

Our runs are surely well thermalized for $L \leq 7$: for each copy β has visited all possible values at least a few times, and the system has never been stuck. $L = 9$ is more delicate, and we are not sure that the data points with lower T values are fully thermalized: we have repeated different trial runs, with different values of the parameters, and the one we report here are those that turn out to be better thermalized. The differences among the different runs were mainly minor, and a possible remanence of on thermalization effects would affect only minor issues that we will point out in the following. Here we will only insist on features that are surely representing thermal equilibrium even on the $L = 9$ lattice.

3. Spin-glass susceptibilities

In this section we will discuss the overlap and the energy overlap susceptibilities. We will show the signature of a spin-glass-like phase transition. We will discuss the location of the critical temperature and the determination of the critical exponents.

We consider two real replicas of the system with spins σ_i and τ_i , and the local energy operator

$$\epsilon_i^{(\sigma)} \equiv \frac{1}{2D} \sigma_i \sum_j J_{i,j} \sigma_j \quad (2)$$

where the sum runs over first neighbours of the site i (on a 4D hypercubic lattice of linear size L and volume $V = L^4$). The *overlap* operator is defined as

$$q \equiv \frac{1}{V} \sum_i \sigma_i \tau_i \quad (3)$$

and the *energy overlap* operator as

$$q_E \equiv \frac{1}{V} \sum_i \epsilon_i^{(\sigma)} \epsilon_i^{(\tau)}. \quad (4)$$

This operator plays a crucial role, since it allows us to distinguish a possible trivial RSB from a non-trivial breaking. In the mean-field RSB q_E and q^2 coincide, while a non-trivial behaviour of q induced by the presence of interfaces would generate a trivial q_E . Detecting a non-trivial behaviour of q_E is strong evidence for a RSB-like behaviour. We will consider the probability distribution of the overlap for a given sample of the quenched disorder, $P_J(q)$, and the same for the energy overlap, $P_J^E(q)$. We will call $P(q)$ and $P^E(q)$ the probability distribution integrated over the quenched disorder.

We define the *overlap susceptibility* as

$$\chi_q \equiv V(E(q^2) - E(q)^2) \quad (5)$$

where by $E(\cdot)$ we denote the combined operation of a thermal average and an average over the quenched disorder J (in the usual notation $E(\cdot) = \overline{\langle \cdot \rangle}$). We define the *energy overlap susceptibility* as

$$\chi_{q_E} \equiv V(E(q_E^2) - E(q_E)^2). \quad (6)$$

In figure 1 we plot the overlap susceptibility χ as a function of T for $L = 3, 5, 7$ and 9, and in figure 2 we plot the energy overlap susceptibility χ_E . The statistical errors are computed using a jack-knife algorithm.

Both susceptibilities show a divergence in the low T region. The comparison of figure 1 with the analogous plot of [20] shows a difference: we do not see a cusp but a clear divergence (not only for $L = 7$ but also for $L = 9$ down to $T = 1.0$). We believe this is

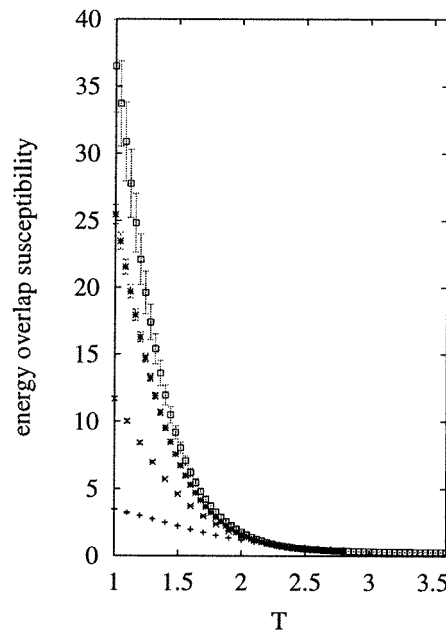
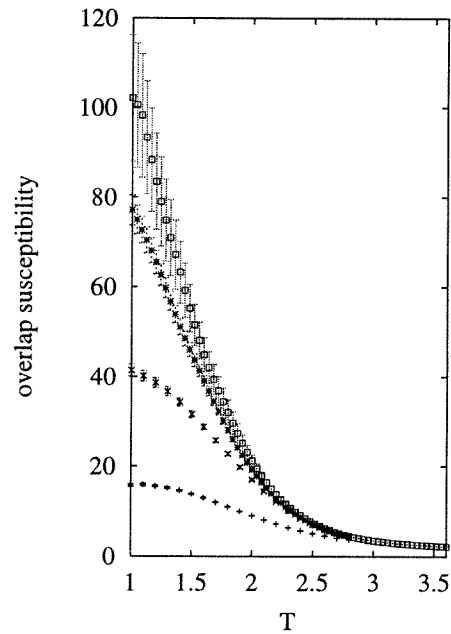


Figure 1. χ as a function of T . Open squares: $L = 9$, asterisks: $L = 7$, crosses: $L = 5$ and horizontal bars: $L = 3$. **Figure 2.** As in figure 1 but for χ_{qE} .

very well explained from some non-complete thermalization for the larger lattices of [20] (this possibility is proposed and discussed in [20] itself: a non-complete thermalization has exactly the effect of smoothing the divergence, since correlations on large scale cannot be created): these measurements are very delicate. As we have already discussed we are completely safe as far as the $L = 7$ lattice is concerned, but $L = 9$ was clearly our limit. It is important to stress that this is the only point of discrepancy with [20]: as far as other (less sensitive) quantities are concerned (and even for the susceptibility on the two smaller lattice sizes) we find exactly the same results. However, [20] does not analyse the quantities based on the energy overlap.

As we have said, the divergence of the two susceptibilities is clear. We are able to follow the divergence on thermalized lattices down to $T = 1.0$. The fact that the energy overlap susceptibility also diverges makes a stronger case for a RSB-like spin-glass phase. The analysis of [21] hints that at $h = 0.4$ is close or slightly lower than 1.5. We just note at this point that the data of figures 1 and 2 are fully compatible with this value.

In figures 1 and 2 one can see that there is a temperature region where the behaviour is asymptotic (i.e. measurements on the $L = 9$ lattice are compatible with those taken on smaller lattices). We use this region to fit the susceptibility as a function of the reduced temperature $\frac{T}{T-T_c}$, with

$$\begin{aligned}\chi_q(t) &\simeq A_q t^{-\gamma} \\ \chi_{qE}(t) &\simeq A_{qE} t^{-\gamma_\epsilon}.\end{aligned}\tag{7}$$

We will use the value $T_c = 1.4$ (in agreement with the results of [21] and with evidence that will be discussed later in this note). The fits in the region of T going from 2.1 to 2.6 (that we show in figure 3) give $\gamma = 1.97$ and $\gamma_\epsilon = 1.93$. χ_q has a stronger L dependence

than χ_{qE} . We plot in figure 3 the logarithm of χ_q and χ_{qE} versus $\log(t)$, and the best fits to the form (7).

The conclusion of this analysis is that the numerical data are compatible with a divergence at $T_c \simeq 1.4$ with an exponents γ and γ_ϵ close to 2. It is interesting to notice that the zero-field exponents from [24] and references therein found a value of γ very similar to our value in field.

We have also carried out a standard finite-size scaling analysis, by selecting T_c and the critical exponents in such a way that curves at different lattice size collapsing together as well as possible. As usual for not very accurate data (as is unfortunately frequently the case for numerical simulations of complex systems) this analysis does not give unambiguous results, but only hints reasonable and preferred set of values. We use for χ_q the leading scaling form

$$\chi_q = L^{\frac{\gamma}{\nu}} \bar{\chi}_q (L^{\frac{1}{\nu}} (T - T_c)) \tag{8}$$

and the same form for χ_{qE} . By looking at χ_q we find that $T_c = 1.4$, $\frac{1}{\nu} = 0.7$ and $\frac{\gamma}{\nu} = 1.3$ give a very good fit. The same values (with $\gamma_\epsilon = \gamma$) also give a very good scaling behaviour for χ_{qE} .

If one took a higher value of T_c (that could be suggested by a possible interpretation of the crossover regime we will discuss in the next section, but is discouraged by the dynamical data of [21]), for example $T_c = 1.8$, we would find a higher value of ν , of the order of 2, and $\frac{\gamma}{\nu} \simeq 1$. Again, the finite-size scaling analysis and the study of the asymptotic T dependence would be consistent at this effect.

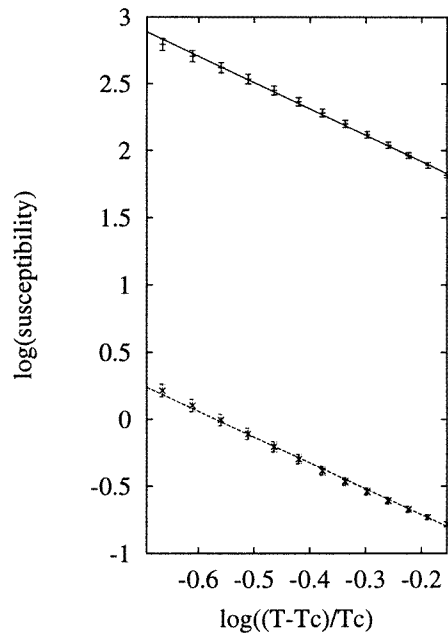


Figure 3. $\text{Log}(\chi_q)$ and best fit to a power law (full line) and $\text{log}(\chi_{qE})$ and best fit to a power law (broken line) versus the logarithm of the reduced temperature.

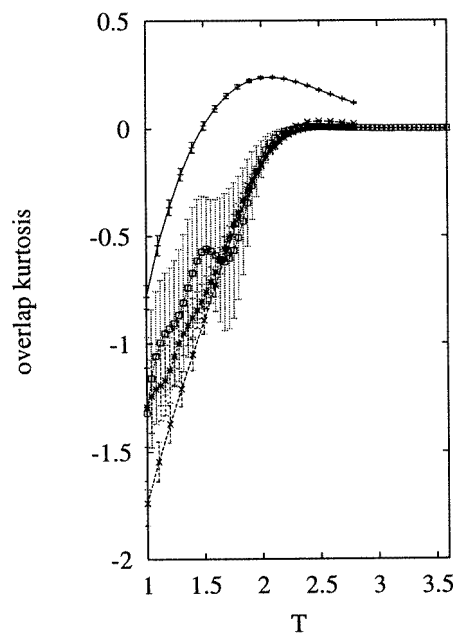


Figure 4. As in figure 1 but for the overlap kurtosis g .

4. Skewness and kurtosis

In order to qualify the probability distribution of the overlap and of the energy overlap we will define and analyse their kurtosis (the Binder cumulant) and their skewness. For zero-field deterministic and disordered statistical systems the Binder cumulant g of the order parameter is a very good signature of the phase transition: curves of g versus T cross at the critical point, since the kurtosis of the probability distribution of the order parameter at the critical point is an universal quantity. In the infinite volume limit g goes to 0 in the warm phase: it goes to 1 in a ferromagnetic phase, and to a non-trivial function in the broken phase of the Parisi RSB solution of the mean-field spin glass theory.

Here, since we have a non-zero magnetic field, we have to consider connected expectation values. We define the overlap kurtosis on a lattice of linear size L as

$$g(T) \equiv \frac{3}{2} - \frac{1}{2} \frac{E((q - E(q))^4)}{E((q - E(q))^2)^2} \equiv \frac{3}{2} - \frac{1}{2} \frac{\chi_q^{(2)}}{\chi_q^2} \quad (9)$$

which defines $\chi_q^{(2)}$. We define the kurtosis for the energy overlap g_ϵ in the analogous way, by using q_E . We define the skewness of the probability distribution of the overlap as

$$s(T) \equiv \frac{E((q - E(q))^3)}{E((q - E(q))^2)^{3/2}} \equiv \frac{\chi_q^{(3/2)}}{\chi_q^{3/2}} \quad (10)$$

which defines $\chi_q^{(3/2)}$. In the definition of the skewness of the energy overlap probability distribution s_ϵ one substitutes q_E into q . We note now that the study of the q_E probability distribution turns out to be very important. We plot $g(T)$ for the four different lattice volumes in figure 4). In this and following plots errors are from sample-to-sample fluctuations evaluated with a jack-knife analysis.

The difference with the usual zero-field picture is strong. There is a clear change of regime close to $T = 2$ (the critical point at $h = 0$). The $L = 3$ system is small and different, and never really Gaussian in our T range. For $L \geq 5$ g becomes non-trivial when T becomes smaller than 2. The q -kurtosis in this region does not change much with size. In the statistical error the values of the $L = 5, 7$ and 9 lattice are compatible (but maybe at $T \simeq 1$ where also small non-equilibrium effects have to be accounted for). The fact that the kurtosis only has a small L dependence (that we do not see but could be hidden by the large statistical errors) and is non-trivial is very clear from our data. Again, the traditional crossing behaviour is completely absent (likely even in the infinite-volume limit) in our data. Two things must be stressed here: first, that the existence or non-existence of a crossing also depends from the shape of the critical asymptotic probability distribution, and second that we cannot exclude, and on the contrary we clearly detect (see for example figure 5) the existence of very strong finite-size effects.

Figure 5, where we plot the energy overlap kurtosis, is dramatically and delightfully different from figure 4. It is already very interesting to look at the high T region: here only the $L = 9$ lattice starts to be Gaussian, while smaller lattices have a strongly non-Gaussian behaviour. In the cold region again there is a strong finite-size dependence (in the next section we will see that there is a finite-size double peak structure that is disappearing on large lattices). Here there is a crossing, even if it is inverted as compared with usual, $h = 0$ systems, where in the warm phase the kurtosis curves become lower with increasing lattice size: in our case for small sizes and high T we have a negative kurtosis, that tends to zero from below when the size increases. This real, inverted crossing is at T higher than 1.5, but we believe it should be taken *cum grano salis* as far as the exact determination

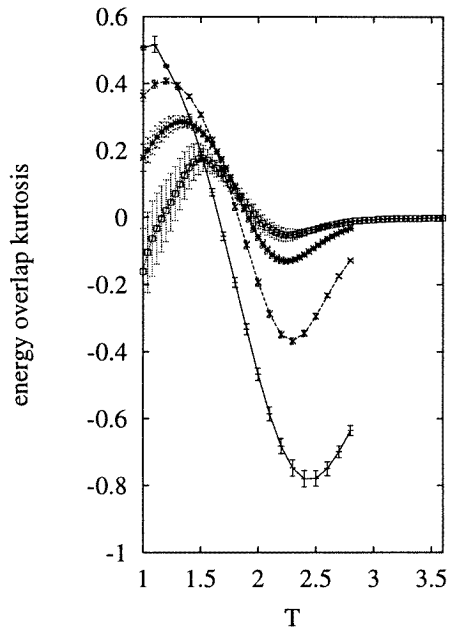


Figure 5. As in figure 1 but for the energy overlap kurtosis g_ϵ .

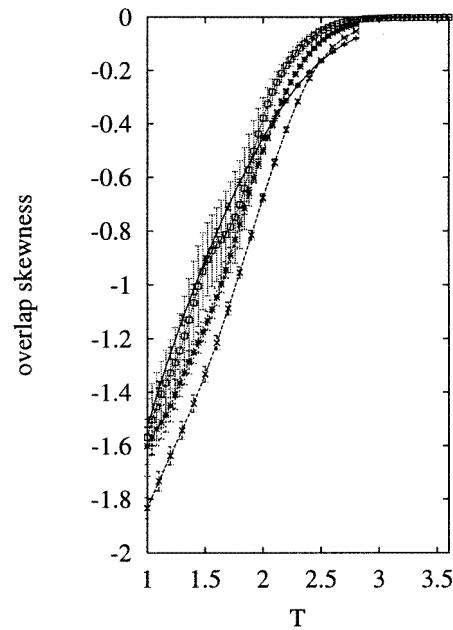


Figure 6. As in figure 1 but for the overlap skewness s .

of the critical point is concerned. The finite-size effects make themselves clear in the non-Gaussian behaviour in the warm phase, and in a peak in the cold phase, that shrinks and shifts with increasing lattice size (see figure 5). A value of $T_c \simeq 1.5$ is very compatible with this picture.

The behaviour of the skewness for the overlap (figure 6) and for the energy overlap (figure 7) repeats a similar pattern. We find a symmetric behaviour of the overlap in the warm phase, and curves collapse to a non-trivial shape in the low T regime. The energy overlap skewness, on the contrary, starts to become zero in the warm region only on our larger lattice, $L = 9$, and heavily depends on L in the low T region. Again a peak close to $T \simeq 2$ is shrinking with increasing lattice size.

In the next section we will discuss the full probability distribution. The analysis we have discussed here strongly suggests the existence of a RSB phase. We have been able to get hints for the value of T_c and of the critical exponents, but such estimates, that surely improve on existing ones, have to be considered only as hints.

5. Probability distributions

Before starting a detailed discussion of the behaviour of the probability distribution of the order parameter for a given sample $P_J(q)$ and of the disorder averaged $P(q)$ we briefly discuss finite-size effects on, for example, $\langle q \rangle_L$. We have analysed the size dependence of $\langle q \rangle_L$ and $\langle q_E \rangle_L$.

We notice here that the probability distributions that we show in figures 10–13 (and that we will discuss better in the following) make clear the presence of strong finite-size effects affecting the mean value of the overlap.

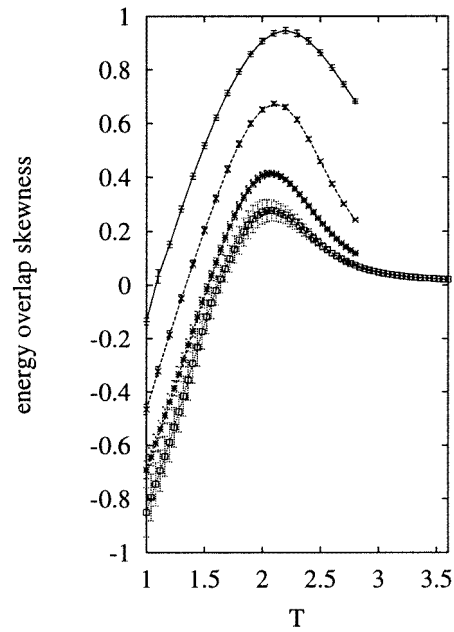


Figure 7. As in figure 1 but for the energy overlap skewness s_e .

We have tried a fit of the type (see [17] for a detailed discussion of the issue)

$$\begin{aligned} \langle q \rangle_L &\simeq \langle q \rangle_\infty + \frac{A}{L^{d_q}} \\ \langle q_E \rangle_L &\simeq \langle q_E \rangle_\infty + \frac{A_E}{L^{d_{q_E}}}. \end{aligned} \quad (11)$$

In the Parisi solution of the mean-field theory $d_q = d_{q_E}$: corrections that scale as $V^{-1/3}$ and the fact that the upper critical dimension is 6 imply that in the mean-field limit we expect $d_q = 2$. As a function of the exponents γ and ν one has that $2d_q = 4 - \gamma/\nu$.

We find that for the overlap the best fit to d_q (using $L = 3, 5, 7$ and 9) increases with T from 2.3 ± 0.5 at $T = 1.0$ to 3.2 ± 0.2 at $T = 1.6$, and to a number larger than 4 for T among 2 and 3 (for $T > T_c$ we expect an exponential decay, but on a finite lattice with a finite number of points we can fit an effective exponent). d_{q_E} is larger: here finite-size effects are smaller, and the exponent more difficult to determine. In the region of $T = 1.6, 1.8, 2.0$ we find an exponent close to 4, that increases in the high T region. For example at $T = 1.6$, that asymptotically is probably marginally off-critical but very close to the estimated T_c , where we have a clear determination of both exponents, we have a ratio $\frac{d_{q_E}}{d_q} \simeq \frac{4}{3}$ (to be compared with the 1 that one finds in the mean-field theory). The behaviour of $\langle q \rangle_L$ does not look compatible with a pure exponential, while $\langle q_E \rangle_L$ would also be compatible with an exponential decay. We stress again that since the expected finite-size corrections have a very complex pattern (different terms could be leading for different L values) the exact theoretical significance of this numerical result is not clear (see [17] for a discussion), but for the fact that we find that the two exponents are not very different from those that are found in mean field. For a comparison of the equilibrium value $E(q)$, and the dynamical value of the overlap, q_D , see figure 2 of [21] (our data for $E(q)$ are very similar to those of [20]).

Let us examine in further detail now the full $P(q)$ and $P^E(q)$ and the probability distributions for a given sample, $P_J(q)$ and $P_J^E(q)$. In figure 8 we plot $P(q)$ at $L = 9$ for

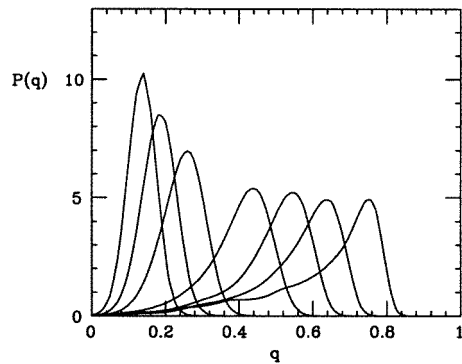


Figure 8. $P(q)$ at $L = 9$ for different T values: from the left are the curves for $T = 2.4, 2.2, 2.0, 1.6, 1.4, 1.2, 1.0$.

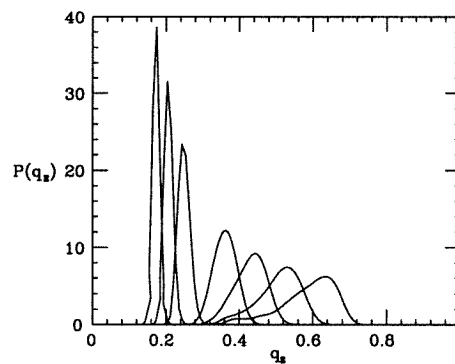


Figure 9. As in figure 8 but for $P^E(q)$.

different T values. At $T = 2.4$ P is Gaussian and symmetric. For lower T values we get a strong deviation from a Gaussian behaviour. We will discuss later the fact that finite-volume effects are very strong (and they turn out to be the most serious limitation in the case of the simulations we are discussing here). We can already notice that at $T = 1$ from the results of [21] we expect that the minimum value allowed for the overlap is $q_{\min} \simeq 0.55$. On the contrary even on our larger size, $L = 9$, we get a long tail that basically goes down to $q = 0$ (we will see later that it goes down to -1 for the smaller lattice sizes).

A very similar pattern holds for $P^E(q)$ in figure 9. Here even at $L = 9$ and at $T = 2.4$ (deep in the warm phase) the probability distribution is not yet fully Gaussian (as one can also see from the kurtosis and the skewness). As for $P(q)$ the distribution becomes very asymmetric at low T , with a large tail towards small overlaps.

It is interesting to analyse in more detail the size dependence of the probability distributions. In figure 10 we show $P(q)$ versus q at $T = 2.0$ for $L = 3, 5, 7$ and 9 . This is the point of the transition in the $h = 0$ model, asymptotically in the warm region for $h = 0.4$. Clearly for $L = 3$ the distribution is far from Gaussian: only at $L = 7$ one sees a Gaussian behaviour.

The same function at low T is very different. We show $P(q)$ versus q at $T = 1.0$ in figure 11. Also, here finite-size effects are very large, but $P(q)$ does not show any sign of convergence to a Gaussian behaviour. In the mean-field RSB solution one would expect a δ -function at q_{\min} (that, as we already said, at $T = 1.0$ is close to 0.55 [21]): here, at least for $L < 9$, we do not see a δ -function-like contribution at $q < q_{\max}$. Only at $L = 9$ we see a small bump at $q \simeq 0.2$: we see it in all our different runs, but we cannot exclude (and on the contrary we believe it is possible) that it is due to a lack of complete thermalization of the $L = 9$ data at the lower T values (as we have discussed even if quantities such as $\langle q^2 \rangle$ are well behaved and apparently thermalized we cannot completely exclude a very small effect of this kind). Also we will discuss a similar effect, that turns out to be due to the finite size of the lattice, for the energy overlap.

In figure 12 we show $P_E(q_E)$ versus q at $T = 2.0$ for $L = 3, 5, 7$ and 9 . Again, on small lattices even at warm T P_E is not symmetric (the tail is in this case for large values of the overlap).

In figure 13 we show that in the cold region ($T = 1$) the energy overlap has even stronger finite-size effects than the spin-spin overlap. Here a spurious peak at low values

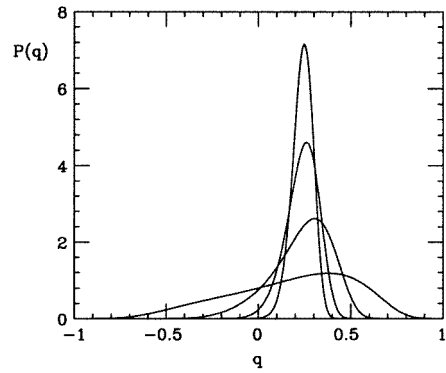


Figure 10. $P(q)$ versus q at $T = 2.0$ for $L = 3, 5, 7$ and 9 (curves from bottom to top).

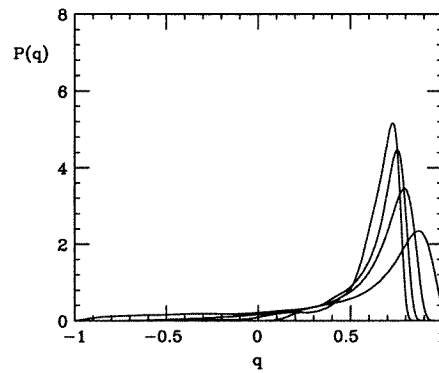


Figure 11. As in figure 10 but $T = 1.0$.

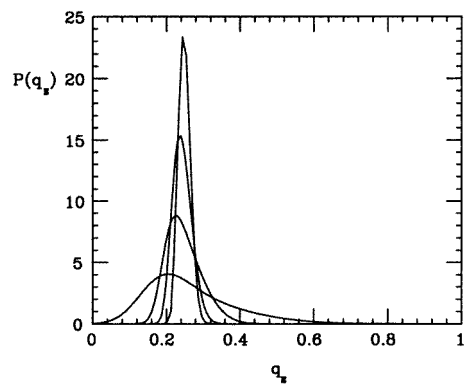


Figure 12. As in figure 10 but P_E .

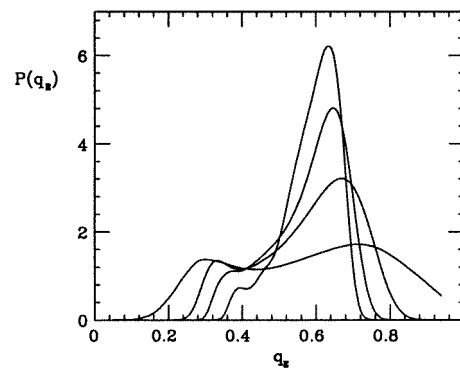


Figure 13. As in figure 10 but P_E and $T = 1.0$.

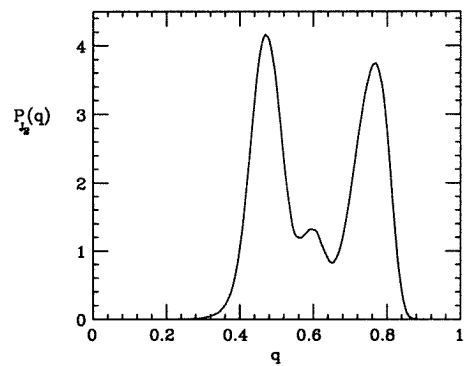


Figure 14. A first $P_I(q)$ for one disorder sample, $L = 9$ and $T = 1$.

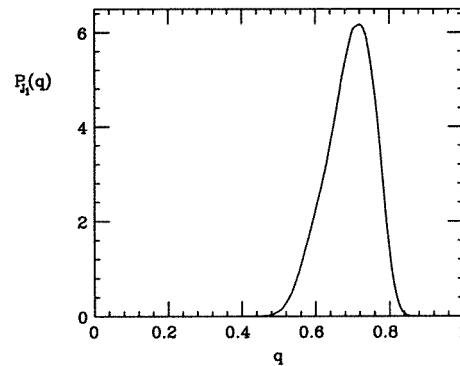


Figure 15. A second $P_I(q)$ for a different disorder sample, $L = 9$ and $T = 1$.

of q_E is very strong for small L values (it carries 30% of the weight at $L = 3$), and becomes smaller and smaller on larger lattices.

We also show, in figures 14 and 15 two individual $P(q)$ for two different realizations

of the quenched disorder at $L = 9$, $T = 1$. It is clear that different samples can have a very different equilibrium probability distribution, and the system does not look self-averaging. In the two examples we show, for example, that it is clear that, like in mean-field theory, we can find systems with one maximum of $P(q)$ and systems with a complex structure of $P(q)$, with many local maxima. The integrated $P(q)$ is not originated from a trivial sum of very similar individual $P_J(q)$, but from the sum of individual very different distributions. It is clear that this feature, crucial in the RSB mean field picture, is shared by the finite-dimensional system in a non-zero magnetic field.

6. Conclusions

We have discussed accurate numerical simulations of the 4D Edwards Anderson spin glass in magnetic field. Our results hint very strongly the existence of a spin glass phase transition. Susceptibilities grow strongly at low T , and fits to a divergent behaviour are very good. Cumulants of the overlap and energy overlap probability distribution such as the kurtosis and skewness show a clear change of regime in the region of temperatures lower than the $h = 0$ critical point. Finite-size effects are dominated by power laws that are similar to those of the mean-field theory. Probability distributions are non-trivial in the low T region, and, what is most important, different samples clearly behave in very different ways. The energy overlap follows the usual overlap in this RSB-like behaviour, making the possibility of a non-trivial behaviour caused by interfaces quite unpalatable.

This work substantiates the results of [21, 22]: we are using here a very different approach (since we look at systems at thermal equilibrium, while these two papers look at systems out of equilibrium). Apart from the discrepancy about the susceptibility (clearly due, in our view, to a marginal lack of thermalization of [20]) our raw data mainly agree, where in common, with those of [20], but our larger statistical sample gives us the possibility of a better precision.

There are also differences with the usual RSB-like approach at $h = 0$. For example here the Binder cumulants do not cross (and the pictures of the $P(q)$ show why). What is more impressive and relevant is the presence of very strong finite-size effects (even on lattices of size $L^4 = 9^4$, that had never before been thermalized in a numerical simulation). These effects are far larger than in the $h = 0$ case. These are the most important limitations of the present numerical simulation (and of the physics conclusions one can draw from them): when finite-size effects are as strong as we have shown is very difficult to be sure that any asymptotic behaviour has been observed. Owing to this all the quantitative results we quote for critical exponents and temperatures have to be taken as simple indications. The other real problem, as far as the coincidence with the RSB mean-field approach is concerned, is that even for $L = 9$ we do not see any trace of a δ -function at $q = q_{\min}$: even if on theoretical grounds we expect this peak to be smaller than the one at q_{\max} [17], and if we know that finite-size effects are very strong, and if we have a small bump in $P(q)$ at $L = 9$ at low q (that we cannot take too seriously), this a worrying point, that is there to demand further clarification.

Acknowledgments

We thank Giorgio Parisi and Felix Ritort for many helpful conversations.

References

- [1] Edwards S F and Anderson P W 1975 Theory of spin glasses *J. Phys. F: Met. Phys.* **5** 965
- [2] Sherrington D and Kirkpatrick S 1975 Solvable model of a spin-glass *Phys. Rev. Lett.* **35** 1793
Kirkpatrick S and Sherrington D 1978 Infinite-ranged models of spin-glasses *Phys. Rev. B* **17** 4384
- [3] de Almeida J R L and Thouless D J 1978 Stability of the Sherrington-Kirkpatrick solution of a spin glass model *J. Phys. A: Math. Gen.* **11** 983
- [4] Parisi G 1979 *Phys. Lett.* **73A** 203
Parisi G 1979 *Phys. Rev. Lett.* **43** 1754
Parisi G 1980 *J. Phys. A: Math. Gen.* **13** L115
Parisi G 1980 *J. Phys. A: Math. Gen.* **13** 1101
Parisi G 1980 *J. Phys. A: Math. Gen.* **13** 1887
Parisi G 1983 *Phys. Rev. Lett.* **50** 1946
- [5] McMillan W L 1984 *J. Phys. C: Solid State Phys.* **17** 3179
Fisher D S and Huse D A 1986 *Phys. Rev. Lett.* **56** 1601
Fisher D S and Huse D A 1988 *Phys. Rev. B* **38** 386
Bray A J and Moore M A 1986 *Glassy Dynamics and Optimization* ed J L van Hemmen and I Morgenstern (Berlin: Springer)
- [6] Marinari E, Parisi G and Ruiz-Lorenzo J J 1997 Numerical simulations of spin glass systems *Spin Glasses and Random Fields* ed P Young (Singapore: World Scientific)
- [7] Sourlas N 1986 Dynamical behavior of three-dimensional Ising spin glass *Europhys. Lett.* **1** 189
- [8] Sourlas N 1988 Three-dimensional Ising spin glasses and ergodicity breaking *Europhys. Lett.* **6** 561
- [9] Caracciolo S, Parisi G, Patarnello S and Sourlas N 1990 3d Ising spin glasses in a magnetic field and mean field theory *Europhys. Lett.* **11** 783
- [10] Caracciolo S, Parisi G, Patarnello S and Sourlas N 1990 Low temperature behavior of 3-D spin glasses in a magnetic field *J. Physique* **51** 1877
- [11] Huse D A and Fisher D S 1991 On the behavior of Ising spin glasses in a uniform magnetic field *J. Physique* **1** 621
- [12] Caracciolo S, Parisi G, Patarnello S and Sourlas N 1991 On computer simulations for spin glasses to test mean field predictions *J. Physique* **1** 627
- [13] Grannan E R and Hetzel R E 1991 Susceptibility of two-, three-, and four-dimensional spin glasses in a magnetic field *Phys. Rev. Lett.* **67** 907
- [14] Singh R R P and Huse D A 1991 *J. Appl. Phys.* **69** 5225
- [15] Kawashima N and Ito N Critical behavior of the three-dimensional $\pm J$ model in a magnetic field *J. Phys. Soc. Japan*
- [16] Badoni D, Ciria J C, Parisi G, Pech J, Ritort F and Ruiz-Lorenzo J J 1993 *Europhys. Lett.* **21** 495
- [17] Ciria J C, Parisi G, Ritort F and Ruiz-Lorenzo J J 1993 The de Almeida-Thouless line in the four dimensional Ising spin glass *J. Physique* **3** 2207
- [18] Picco M and Ritort F 1994 Numerical study of the Ising spin glass in a magnetic field *J. Physique* **4** 1619
- [19] Andersson J O, Mattsson J and Svedlindh P 1994 *Phys. Rev. B* **49** 1120
- [20] Picco M and Ritort F 1997 Tempering simulations on the four dimensional $\pm J$ Ising spin glass in a magnetic field *Preprint cond-mat/9702041*
- [21] Marinari E, Parisi G and Zuliani F 1998 4D spin glasses in magnetic field have a mean field like phase *J. Phys. A: Math. Gen.* **3** 1181
- [22] Parisi G, Ricci-Tersenghi F and Ruiz-Lorenzo J J 1997 On the dynamics of the 4d spin glass in a magnetic field *Preprint cond-mat/9711122*
- [23] Marinari E and Parisi G 1992 *Europhys. Lett.* **19** 451
Tesi M C, van Rensburg E J, Orlandini E and Whillington S G 1992 *J. Stat. Phys.*
Hukushima K and Nemoto K 1996 *J. Phys. Soc. Japan* **65** 1604
Marinari E 1996 *Optimized Monte Carlo Methods (Lectures Given at the 1996 Budapest Summer School on Monte Carlo Methods)* ed J Kertesz and I Kondor (Berlin: Springer) to be published
- [24] Klein L et al 1991 *Phys. Rev. B* **43** 11249